# Exploring the mechanism(s) of energy dissipation in the light harvesting complex of the photosynthetic algae *Cyclotella meneghiniana* ☆

Charusheela Ramanan [a,*,1], Rudi Berera [a,**,1], Kathi Gundermann [b], Ivo van Stokkum [a], Claudia Büchel [b], Rienk van Grondelle [a]

[a] *Division of Biophysics, Department of Physics and Astronomy, Faculty of Sciences, VU University Amsterdam, The Netherlands*
[b] *Institute of Molecular Biosciences, Goethe University Frankfurt, Frankfurt, Germany*

## ARTICLE INFO

## ABSTRACT

Photosynthetic organisms have developed vital strategies which allow them to switch from a light-harvesting to an energy dissipative state at the level of the antenna system in order to survive the detrimental effects of excess light illumination. These mechanisms are particularly relevant in diatoms, which grow in highly fluctuating light environments and thus require fast and strong response to changing light conditions. We performed transient absorption spectroscopy on FCPa, the main light-harvesting antenna from the diatom *Cyclotella meneghiniana*, in the unquenched and quenched state. Our results show that in quenched FCPa two quenching channels are active and are characterized by differing rate constants and distinct spectroscopic signatures. One channel is associated with a faster quenching rate ($16\ ns^{-1}$) and virtually no difference in spectral shape compared to the bulk unquenched chlorophylls, while a second channel is associated with a slower quenching rate ($2.7\ ns^{-1}$) and exhibits an increased population of red-emitting states. We discuss the origin of the two processes in the context of the models proposed for the regulation of photosynthetic light-harvesting. This article is part of a Special Issue entitled: Photosynthesis Research for Sustainability: Keys to Produce Clean Energy.

© 2014 Elsevier B.V. All rights reserved.

## 1. Introduction

In order to cope with the deleterious effects of excess light illumination and more generally as a response to unfavorable growth conditions, photosynthetic organisms have developed protective strategies generally known as non-photochemical quenching (NPQ). While the process has been the subject of extensive investigation in plants [1,2], much less research has been devoted to understanding NPQ in algae. In plants, four mechanisms involving either chlorophyll–carotenoid [3–7] or chlorophyll–chlorophyll interaction [8,9] have been proposed to be (partly) responsible for energy dissipation. Increasing evidence has recently emerged pointing to charge-transfer states as key players in the regulation of photosynthetic light-harvesting [4–6,10,11].

Diatoms are unicellular photosynthetic organisms with light-harvesting systems termed fucoxanthin–chlorophyll proteins (FCP) due to the prominence of the fucoxanthin (Fx) carotenoid [12]. FCPs demonstrate high homology to the LHCII antennae of higher plants, with some

distinct differences, particularly in pigment composition [13,14]. These diatom light-harvesting antennae contain chlorophyll a (Chl *a*), as in plants, but in addition they bind Chl *c* rather than the Chl *b*. Furthermore, there is a higher ratio of carotenoids, with four Fx per four Chl *a* and one Chl *c* [15]. In addition to the Fx carotenoid, diadinoxanthin (Dd) and diatoxanthin (Dt) are bound in sub-stoichiometric amounts. Under high light conditions, Dd is converted to Dt, which further correlates with a build-up of NPQ, analogous to the xanthophyll cycle in plants [16–19]. Finally, the Fx carotenoid contains a carbonyl group on the conjugated backbone, resulting in an intramolecular charge transfer (ICT) state which is coupled with the first excited singlet state $S_1$, causing the excited state dynamics to depend strongly on the polarity of the environment [20,21].

Not only the pigment complement, but also the polypeptides and the supra-molecular arrangement of FCPs show some differences compared to the organization of the antennae in higher plants. In the diatom *Cyclotella meneghiniana* two main FCPs can be found, differing in polypeptide composition as well as in oligomeric state. FCPa is a trimeric complex composed of different Lhcf and Lhcx polypeptides, whereas FCPb is a higher oligomer built from probably nine identical Lhcf subunits [13,19]. Lhcf polypeptides are a group of Lhc proteins thought to be involved mainly in light-harvesting, whereas Lhcx proteins were proven to be involved in photoprotection [22]. In line with this, several spectroscopic in vitro studies demonstrated reduced fluorescence yield of FCPa complexes under conditions that promote NPQ in vivo, such as

  \* Corresponding author. Tel.: +31 20 59 82869.
 \*\* Corresponding author. Tel.: +31 20 59 87426.
    *E-mail addresses:* c.ramanan@vu.nl (C. Ramanan), r.berera@vu.nl (R. Berera).
  [1] These authors contributed equally to this work.

high diatoxanthin content, low pH and especially aggregation of the FCPa complexes [11,23,24].

Diatoms possess highly efficient NPQ, stronger than in any terrestrial plants [18,25,26]. This process has been explored in various diatoms by biochemical and spectroscopic techniques [11,16,18,22,23,27–35]. These studies have demonstrated the essential role of Lhcx, noted above, as well as the accumulation of diatoxanthin [18], akin to the accumulation of zeaxanthin in higher plants. Spectroscopic studies both in vivo and in vitro point towards multiple quenching processes/sites in FCPs [24,29,30,35], though the time-scales of the quenching and exact molecular mechanisms involved remain under investigation.

In order to obtain further insight into the biophysical mechanisms underlying the photoprotective energy dissipation in diatoms, we applied transient absorption spectroscopy [36] to FCPa isolated from the diatom *C. meneghiniana*. Previous work, including our own [15], has demonstrated the efficient and fast energy transfer from fucoxanthin and Chl *c* to Chl *a* in FCPs [31,37]. Herein, the complexes were studied in the light-harvesting and dissipative (quenched) states upon selective Chl *a* excitation at 680 nm in order to focus on quenching processes within the Chl *a* pool. We applied global and target analysis techniques [38] to our data and determined the detailed kinetics of the quenching process and the spectroscopic signatures of the quenching species. Our results reveal two quenching processes in FCPa characterized by fast and slow quenching rates and distinct spectroscopic signatures, pointing to the contribution of a charge-transfer state in the photoprotective mechanisms of this diatom.

## 2. Materials and methods

### 2.1. Preparation of FCP complexes

The diatom *C. meneghiniana* (Culture Collection Göttingen, strain 1020-1a) was cultured and FCPa complexes were isolated as previously described [23]. In brief, cells were harvested after growth in modified ASP medium supplemented by 2 mM silica [39] for 7 days under white light (140 µmol photons $m^{-2}$ $s^{-1}$) with a 16 h light/8 h dark cycle at 18C. Thylakoid membranes were isolated by several centrifugation steps after breaking the cells in a bead mill and thylakoids containing 0.5 mg total Chl *a* (0.25 mg/mL) were solubilized for 20 min on ice with 20 mM ß-dodecyl maltoside (ß-DDM, Glykon, Germany) (1 mol Chl *a*: 70 mol ß-DDM). FCPa was then separated by ion exchange chromatography in buffer 1 (25 mM Tris, 2 mM KCl, 0.03% ß-DDM (w/v), pH 7.4) followed by a sucrose gradient ultracentrifugation (27000 rpm, 4 °C) to remove remaining contaminations from photosystems. After preparation, the FCPa complexes were washed once using buffer 1 without ß-DDM and then concentrated using filtration devices with 30 kD cutoff (Centripreps). For the preparation of quenched, i.e. aggregated, FCPs, several steps of dilutions and concentrations were done followed by dialysis against buffer 1 without ß-DDM (38 h, 4 °C). Afterwards, the quenched state of the FCPa samples was adjusted by incubation with 50 mg of bio-beads (SM-2 adsorbent, Bio-Rad), to give samples with fluorescence reduced by a factor of ≈15.

### 2.2. Transient absorption spectroscopy

Femtosecond pulses were obtained from a Ti:sapphire oscillator-regenerative amplifier (Coherent Mira seed and RegA) to obtain ≈80 fs pulses at 800 nm at 40 kHz repetition rate. The beam was split in two, with one path focused on a sapphire disk to generate a white light continuum for the probe beam. The remainder of the 800 nm beam was used to pump an optical parametric amplifier (Coherent OPA) to obtain ≈100 fs pulses centered at 680 nm for the pump beam, focused to a spot size of ≈150 µm. The energy for pulse varied according to the experiment, and is indicated in the results below. The polarization between the pump and probe beams was set at magic angle and the instrument response function was fit to a Gaussian of ≈100 fs

(FWHM). Cuvettes with 2 mm pathlength were used, and all measurements were done at room temperature. The data were analyzed with global analysis techniques to retrieve Evolution Associated Difference Spectra (EADS) which represent in general a mixture of molecular states. In addition, target analysis was done using a specific kinetic scheme to retrieve Species Associated Difference Spectra (SADS), which correspond to pure molecular species [38].

## 3. Results

### 3.1. Steady-state characterization

Fig. 1 shows the steady-state absorption spectra of FCPa in both the solubilized (light-harvesting) and aggregated (quenched) states, hereafter referred to as **sFCPa** and **qFCPa**, respectively. The $Q_y$ absorption band of Chl *a* peaks at 672 nm, while that of Chl *c* is seen in much lower ratio at 636 nm. The broad signal between 475 and 550 nm is due to carotenoid absorption, primarily fucoxanthin and diadinoxanthin, with minor amounts of diatoxanthin [13,19]. The spectra are in agreement with previous reports [31,32]. Relative to **sFCPa**, **qFCPa** demonstrates some broadening in the Soret band as well as a small tail to the red side of the $Q_y$ band. These features are due to aggregate formation and some scattering due to aggregate size.

### 3.2. Transient absorption spectroscopy

Transient absorption spectra were measured for both **sFCPa** and **qFCPa** at $\lambda_{ex} = 680$ nm. The corresponding kinetics monitored at 677 nm are shown in Fig. 2 and demonstrate the shorter excited state lifetime of **qFCPa**, evidenced by the faster recovery of the ground-state bleach (GSB). Transient kinetics of **sFCPa** and **qFCPa** at varying incident pump intensities are shown in Fig. 3, monitored at 677 nm. The kinetics from the 2.5 and 15 nJ/pulse experiments are scaled relative to the 10 nJ/pulse data with scaling factors of 0.18 and 1.62 for **sFCPa** and 0.22 and 1.49 for **qFCPa**. It is readily apparent that the lowest energy data (black trace) decay more slowly over the timescale of the measurement. However, the 10 and 15 nJ/pulse kinetics exhibit very similar behavior. This suggests a linear regime during the first picoseconds for these powers. After 1 ps and up to tens of picoseconds, the 15 nJ/pulse trace (blue) shows the fastest decay, whereas the 10 nJ/pulse traces (red) are intermediate. (Fig. 3b) These power dependent studies indicate that the 2.5 nJ/pulse measurements demonstrate significantly less annihilation character than the 10 and 15 nJ/pulse data.
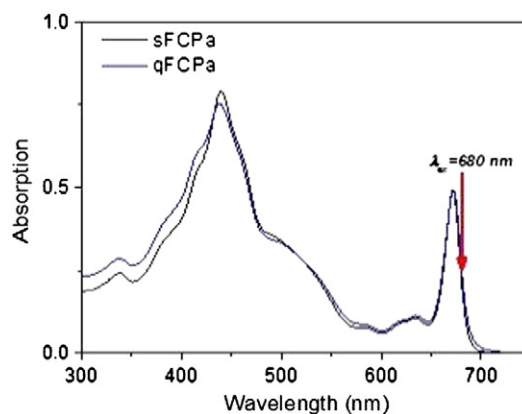


**Fig. 1.** Steady-state absorption of **sFCPa** and **qFCPa** samples for transient absorption. The red arrow indicates the excitation wavelength.
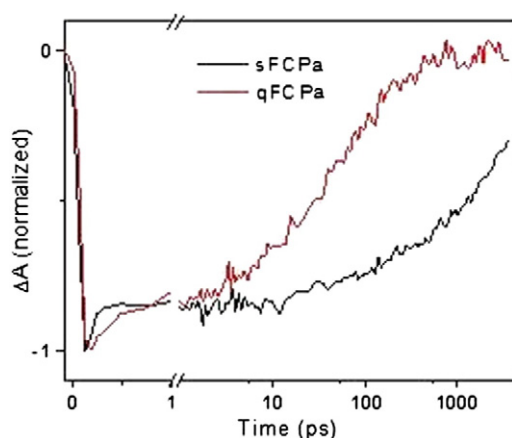
Fig. 2. Transient kinetics of **sFCPa** and **qFCPa** measured at 2.5 nJ/pulse incident power and monitored at 677 nm, demonstrating the recovery of the $Q_y$ GSB.

### 3.3. Global analysis

Global analysis of the transient absorption measurements resulted in the evolution associated difference spectra (EADS) shown in Fig. 4 for 2.5 nJ/pulse incident pump intensity. These traces represent the spectral evolution via a sequential kinetic scheme.

The **sFCPa** sample requires three time components (Fig. 4a) to fit the data. The first (cyan) EADS shows the GSB and stimulated emission (SE) of Chl *a* centered at 675 nm appearing immediately after photoexcitation. The positive features from 600 to 620 nm are most likely due to Raman scatter due to interaction of the pump light with the solvent. This first spectrum decays in 167 fs. This ultrafast component is attributed to vibrational cooling within Chl excited states and equilibration towards bluer absorbing Chls. The spectral shape may also be slightly influenced by a contribution from the coherent artifact. The second (red) EADS also exhibits the negative features associated with GSB and SE, as well as positive features attributed to Chl *a* excited state absorption (ESA). We observe also that due to photoexcitation at the red side of the $Q_y$ absorption, the GSB and SE are blue shifted as a result of uphill energy redistribution. This red spectrum evolves in 111 ps to the final black EADS, which subsequently decays in 3.5 ns. From the red to the black EADS we observe a small loss in the amplitude of the GSB, which we propose to be due to small amount of quenching [35,40,41] and/or annihilation occurring in **sFCPa**. The final 3.5 ns decay reflects the $S_1 \rightarrow S_0$ lifetime of Chl *a* in **sFCPa**.

The EADS of **qFCPa** at this pump intensity also fits well with three components (Fig. 4b). We observe first a fast initial decay reflected by

the evolution from the cyan to the red EADS in 600 fs. Considering the larger energetically connected domain available in the aggregates, it is reasonable that energy redistribution will occur on a slower average timescale hence the longer lifetime of the first EADS in the **qFCPa** compared to **sFCPa**. We thus again attribute this first evolution to vibrational cooling and equilibration, as well as some contribution from a coherent artifact. The resultant red EADS exhibits GSB/SE and Chl *a* ESA features as described above for **sFCPa** and the GSB is also slightly blue shifted following equilibration. This red spectrum decays in 29.6 ps to the black EADS and this process also results in a significant reduction ($\approx 60\%$) of the GSB/SE amplitude. The final black spectrum exhibits similar GSB/SE and ESA features as the other spectra, but also demonstrates an additional feature which manifests on the red side of the SE from $\approx 680$ to 715 nm. This red to black evolution is attributed to extensive energy transfer in the aggregates due to the greater energetic coupling as noted above, which results in increased population of lower energy states and quenching. The black EADS decays in 203 ps. Within the signal-to-noise resolution at this pump intensity, there is no residual signal after the decay of the black spectrum. Thus in **qFCPa** the Chl *a* excited state is completely quenched within hundreds of picoseconds, relative to the 3.5 ns observed for the lifetime of **sFCPa**.

Global analysis was also done for the data with 10 nJ/pulse pump intensity (Supporting Information, Figure S1). At this incident power the signal-to-noise is improved enough that we can survey a larger wavelength region reliably. However, singlet–singlet annihilation must also be taken into consideration. The higher intensity EADS fit to very similar time scales as for the 2.5 nJ/pulse, with faster lifetimes attributed to the contributions from annihilation. Most relevantly, the new negative feature observed in the last **qFCPa** EADS is again present at the higher incident pump power. Also, in the wider spectral window, we are also able to observe the fucoxanthin carotenoid triplet ($^{3*}$Fx) around 560 nm which is formed via quenching of $^{3*}$Chl *a* by Fx [15,42–45]. This is observed in significantly lower amplitude for **qFCPa** than for **sFCPa**, as expected for a quenched complex.

The global analysis of the transient absorption data thus suggests two quenching processes in **qFCPa**, with the observation of a fast and a slow component on the order of tens and hundreds of picoseconds, respectively. Furthermore, the slower process manifests increased energy transfer to redder emitting states, resulting in a distinctive spectral line shape, very different than any of the EADS of the **sFCPa** sample.

### 3.4. Target modeling

In order to disentangle the contributions from quenching and annihilation, and to obtain the spectra of the various states involved in the energy transfer and energy dissipation processes, we applied a target
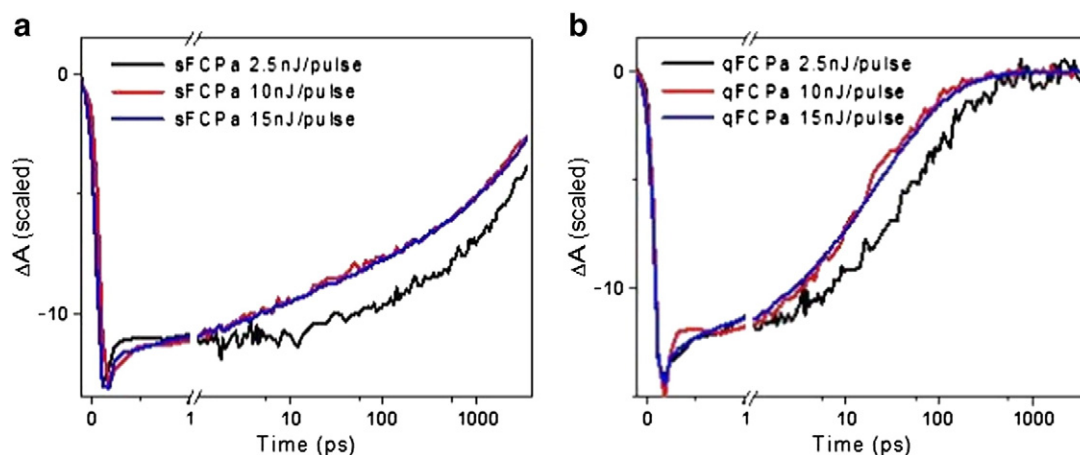


Fig. 3. Transient kinetics of a) **sFCPa** and b) **qFCPa** at varying power intensities monitored at 677 nm.
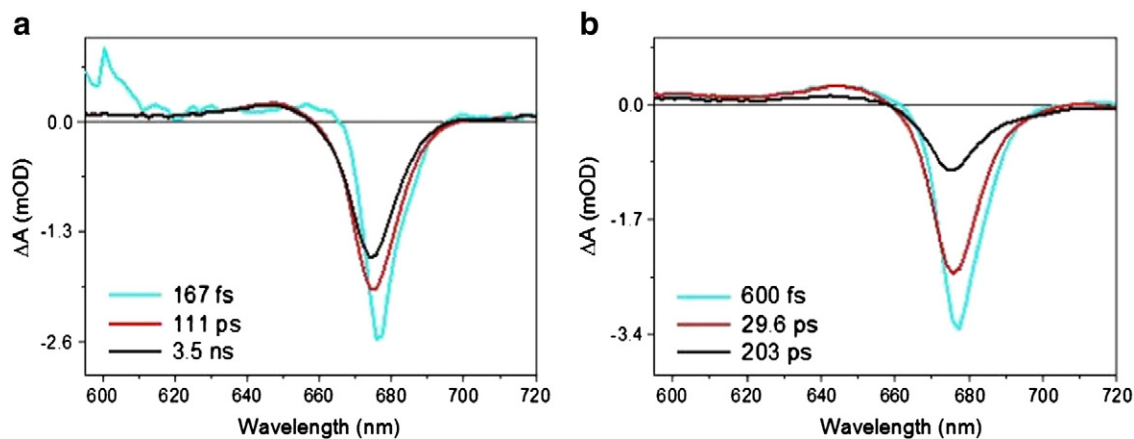
**Fig. 4.** EADS from global analysis of a) **sFCPa** and b) **qFCPa** measured at pump intensity 2.5 nJ/pulse.

analysis to the time resolved data for **qFCPa**. We developed a compartmental model of the kinetic scheme which allows for two independent quenching channels within the Chl a pool, as was suggested from the global analysis. With target analysis we can retrieve the Species Associated Difference Spectra (SADS), which correspond to the spectra of molecular species associated with the respective compartment in the model. The two states are in equilibrium so that the energy can migrate between them. In this and in the subsequent analysis we do not consider a separate compartment for the ultrafast component observed in the global analysis. This allows us to simplify the model in the presence of singlet–singlet annihilation (see below). Also, as all of the signal in **qFCPa** is gone after the second quenching process (within our instrument resolution), no long-lived components, such as those corresponding to (unquenched) singlet and triplet states, are necessary in the target analysis.

The two-state kinetic model is depicted in Fig. 5 along with the SADS estimated from the 2.5 nJ/pulse data. The compartments are representative of sub-populations of the Chl a pool. The initial populations are parameters estimated from the data. The population amplitudes of the compartments are given at particular lifetimes to facilitate interpretation of the decay channels (Table 1). A positive value indicates recovery of a signal, or a decrease in population, whereas a negative value indicates the growth of a signal, or increase in population. Upon photoexcitation, the population resides primarily on Chl 1. At 22 ps we see that

the population of this compartment is decreasing while that of Chl 2 is increasing, due to equilibration within the Chl pool. However, to account for the loss of Chl 1 population, another decay channel must be contributing. Thus, Chl 1 relaxes via both a fast quenching rate $k_{q1} = 27$ ns$^{-1}$ as well as equilibration with Chl 2. At later times, most of the remaining population resides on Chl 2, which decays with. The SADS of Chl 2 exhibits a slightly blue-shifted GSB due to equilibration as well as a significant new contribution from 680 to 715 nm, attributed to the population of redder states.

The fit from the annihilation-free target model describes the relative populations of each compartment from initial excitation through the decay back to ground state. If we consider an arbitrary 100 excitations, then as determined from the populations derived from the fit, 73 excitations populate compartment Chl 1, and 27 populate compartment Chl 2. From the fit we can further see that, 76 excitations are quenched via $k_{q1}$, and 24 via $k_{q2}$. The predominant quenching thus occurs via the fast process, i.e. from the higher energy Chl 1 compartment.

With the addition of a third compartment Chl 1′, we are able to model and quantify the contribution of singlet–singlet annihilation to the data at incident pump powers of 10 and 15 nJ/pulse (Fig. 6). The model was fit simultaneously to all three incident pump powers. The faster quenching rate, $k_{q1}$ was a free parameter limited only to be the same for compartments Chl 1 and Chl 1′. The slower quenching rate $k_{q2}$ was held fixed. Annihilation channels were incorporated for Chl 1
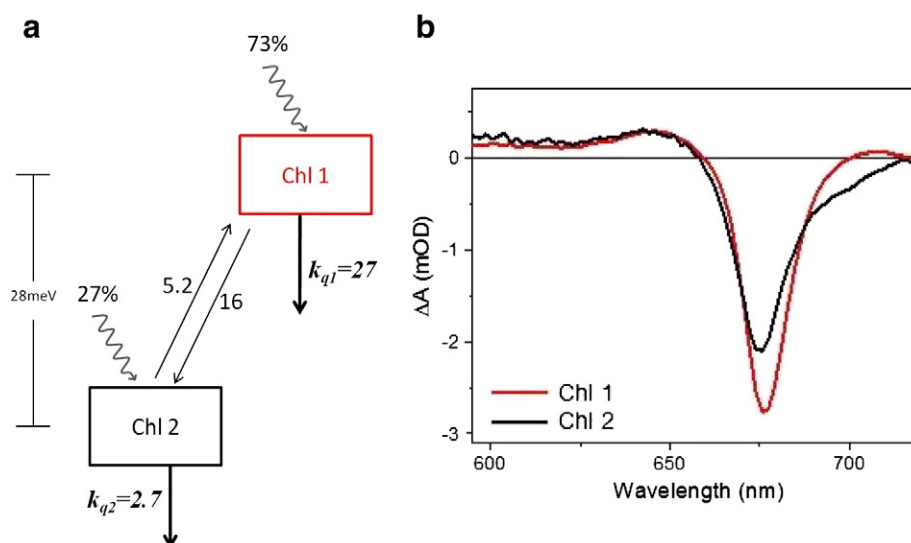


**Fig. 5.** a) Annihilation-free target kinetic model, rate constants in ns$^{-1}$. b) SADS of **qFCPa**, 2.5 nJ/pulse incident pump power.

**Table 1**
Lifetimes with their amplitudes describing the concentrations for the two-compartment model fit to the 2.5 nJ/pulse data of **qFCPa**.

| Lifetime (ps) | 22 | 175 |
|---|---|---|
| Chl 1 | 0.662 | 0.074 |
| Chl 2 | −0.271 | 0.540 |

**Table 2**
Lifetimes with their amplitudes describing the concentrations for the three-compartment model fit to the 2.5 nJ/pulse data of **qFCPa**.

| Lifetime (ps) | 3 | 32 | 196 |
|---|---|---|---|
| Chl 1 | 0.506 | 0.261 | 0.031 |
| Chl 1′ | −0.496 | 0.582 | 0.066 |
| Chl 2 | −0.010 | −0.414 | 0.477 |

and Chl 2. The results shown in Fig. 6 represent the resultant fit values. The quantification of the annihilation for the higher incident pump powers is shown in the SI. Amplitudes of the kinetic fits representing population dynamics are summarized in Table 2. Upon photoexcitation, the population resides primarily on Chl 1. At 3 ps we see a decay of Chl 1 and a concomitant rise in population of Chl 1′, as well as some in Chl 2. This indicates fast equilibration between Chl 1 and 1′, evidenced also by the slight reduction in amplitude and blue-shift of the SADS of Chl 1′ relative to 1. At 32 ps, we see decays of both Chls 1 and 1′ and a rise in Chl 2, indicating equilibration between compartments Chl 1 and 1′ with Chl 2, occurring more slowly than between Chl 1 and 1′. Furthermore, the loss of population in the Chls 1 and 1′ is more than the increase in Chl 2, indicating that part of this decay is due to the fast quenching $k_{q1} = 16$ ns$^{-1}$. Finally, the population resides primarily on the lowest energy compartment Chl 2 and decays with 196 ps. The SADS of Chl 2 is consistent with that in Fig. 5b.

## 4. Discussion

We have recently shown, by making use of Stark fluorescence spectroscopy, that two emitting sites are present in the dissipative state of FCPa and possibly FCPb [11]. From that study, however, we could get little insight into the dynamics of the quenching process and could not put any quantitative basis on it. Our time-resolved work reported here adds an important piece to the understanding of the functioning of FCPs as an energy dissipater. We determined that two quenching channels are present in the dissipative state of FCPa. Our global and target analysis allowed us to extract the kinetics of the two processes, determine their efficiency, and to obtain the transient spectra associated with each of them. The first decay channel is faster with a rate constant of 16 ns$^{-1}$, and is characterized by a spectrum similar to that of the solubilized FCPa but slightly red shifted. The predominant quenching occurs from this channel, which also exhibits GSB/SE features primarily on the red-edge of the $Q_y$ band. Thus the Chl pool associated with this quenching process most likely involves the terminal emitter Chls $a$, populated on multiple timescales.

The second and slower decay channel, with a rate constant of 2.7 ns$^{-1}$, is associated with a spectrum exhibiting increased population of redder states, visible from 680 to 715 nm. These features observed in the slower quenching SADS are in agreement with those observed in the previously mentioned Stark spectroscopy measurements [11]. In that work, the red-shifted emitting band was tentatively attributed to emission from a state resulting from interaction between the fucoxanthin $S_1$/ICT state and the $Q_y$ state of a neighboring Chl $a$. This state was observed to have a low quantum yield of fluorescence and so, if observed in our data, would manifest with a very small negative signal, which is indeed the case. This leads us to propose that the slower quenching process involves the same red-shifted state seen in the Stark experiments. It furthermore strengthens the proposition that a dark state may be involved in its formation. Unlike carotenoids in plants, such as lutein and zeaxanthin, fucoxanthin possesses an ICT state coupled to the $S_1$ state [20,21]. We suggest that the red-shifted state originates from the interaction between the $S_1$/ICT state and one or more Chls $a$ in the FCPa terminal emitter. In addition to the agreement with the Stark fluorescence results, previous work on artificial systems has demonstrated that low-lying carotenoid excited states can couple with a tetrapyrrole $Q_y$ to form energy dissipation channels [46]. As for the driving force behind its formation, at any given time, this interaction could already be present in a small fraction of the solubilized sample. Upon aggregation the increased connectivity of the oligomeric domains would make the red state accessible from trimeric subunits which would otherwise be unquenched under solubilized, i.e. not aggregated, conditions.

It is also possible that a small aggregation-induced conformational change in the terminal emitter is responsible for the formation of the new feature we observed under quenched conditions.

Aggregates of light-harvesting complexes have been studied for decades as a model system for NPQ in plants [47] and more recently in diatoms [11,29,31]. These models have received some criticism since aggregation is regarded as artifactual and not representative of the in vivo physiological environment experienced by the antenna system. However, more recent reports provide increasing evidence that aggregates of light-harvesting antennae can or may be present in vivo [48,49].
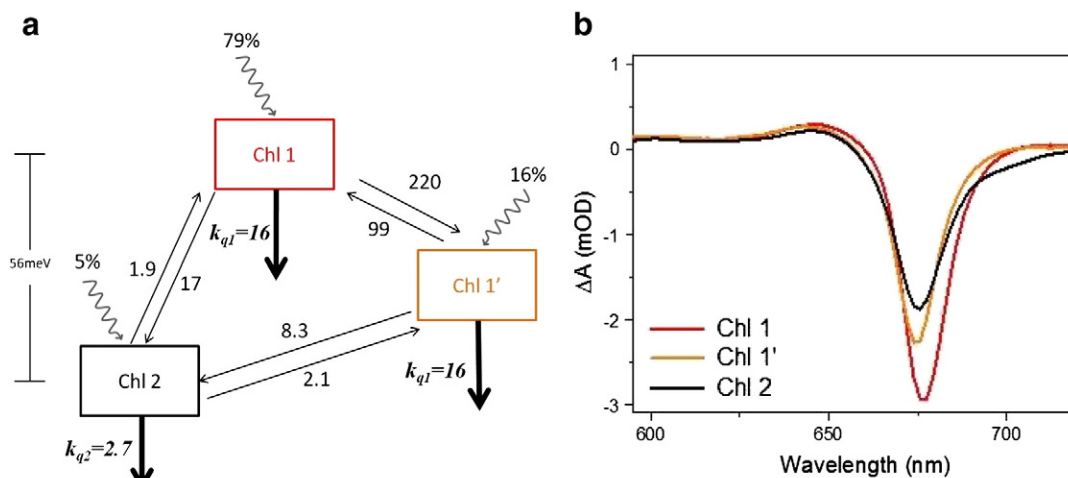


**Fig. 6.** a) Target kinetic model fit to 2.5 nJ/pulse, rate constants in ns$^{-1}$. b) SADS of **qFCPa**, estimated from a simultaneous fit at pump powers of 2.5, 10, and 15 nJ/pulse pump powers.

Recent in vivo studies on *C. meneghiniana* have postulated two NPQ sites with differing functional connectivity [29,30], which lead to the suggestion that quenching occurs partially from aggregated antennae which are associated with PSII and with another quenching process more strongly dependent on diatoxanthin content and occurring in detached antennae. More recent biochemical work has shown that within FCPa quenching occurs as a result of aggregation and diatoxanthin binding [24]. Our results reported here indicate that the two quenching processes suggested for in vivo conditions could take place within the same antenna system.

Contrary to previous reports on photoprotection in other photosynthetic organisms, our results do not demonstrate a carotenoid $S_1$ as a primary quencher for aggregated FCP [4,50]. Given the relatively long lifetime of the fucoxanthin $S_1$/ICT [20] state and the strong quenching in FCP we believe that if energy transfer to the $S_1$/ICT state was a dominant quenching mechanism we would have been able to detect it in our experiments. The suggested contribution from a Fx–Chl charge transfer-type interaction is in agreement with studies of other photosynthetic organisms which point to the role of chlorophyll–carotenoid [3–7] interactions in photoprotective energy dissipation. In particular, carotenoid ICT states have been proposed to be key players in the regulation of photosynthesis [4,6,10,50]. The fact that the interaction proposed here involves not just a carotenoid $S_1$, but the Fx $S_1$/ICT state is important to note, primarily due to the particular energetic nature of this state in Fx and FCP dynamics. Studies have demonstrated multiple spectroscopic forms of Fx in polar environments [51], as well as differing transition dipole moments not only between the $S_1$ and ICT but also for the $S_1$ state itself [21,32]. Furthermore, FCPs demonstrate high heterogeneity in the Fx pool, dependent on growth conditions, and this is also expected to affect any photoprotection process involving Fx [52]. Excitation energy transfer efficiency from Fx to Chl has also been found to vary within the Fx pool [15]. Thus, future studies to characterize the proposed Fx–Chl interaction for photoprotection and the quenching site could give further information regarding the nature and reason for the observed heterogeneities within the Fx pigment composition in FCP.

The existing models for photoprotection in FCP point towards multiple quenching sites and mechanisms. From our results we propose that the predominant and faster quenching process in FCPa occurs distinctly within the Chl pool, while the second and slower one, involves the Fx $S_1$/ICT state which, in cooperation with a nearby Chl, acts as a trap for photoprotective energy dissipation.

## Acknowledgements

## Appendix A. Supplementary data

Supplementary data to this article can be found online at http://dx.doi.org/10.1016/j.bbabio.2014.02.016.

## References

[1] P. Muller, X.P. Li, K.K. Niyogi, Non-photochemical quenching. A response to excess light energy, Plant Physiol. 125 (2001) 1558–1566.
[2] P. Horton, A.V. Ruban, R.G. Walters, Regulation of light harvesting in green plants, Annu. Rev. Plant Physiol. Plant Mol. Biol. 47 (1996) 655–684.
[3] S. Bode, C.C. Quentmeier, P.-N. Liao, N. Hafi, T. Barros, L. Wilk, et al., On the regulation of photosynthesis by excitonic interactions between carotenoids and chlorophylls, Proc. Natl. Acad. Sci. U. S. A. 106 (2009) 12311–12316.
[4] A.V. Ruban, R. Berera, C. Ilioaia, I.H.M. van Stokkum, J.T.M. Kennis, A.A. Pascal, et al., Identification of a mechanism of photoprotective energy dissipation in higher plants, Nature 450 (2007) 575–U22.
[5] T.K. Ahn, T.J. Avenson, M. Ballottari, Y.-C. Cheng, K.K. Niyogi, R. Bassi, et al., Architecture of a charge-transfer state regulating light harvesting in a plant antenna protein, Science 320 (2008) 794–797 (80-.).
[6] R. Berera, C. Herrero, I.H.M. van Stokkum, M. Vengris, G. Kodis, R.E. Palacios, et al., A simple artificial light-harvesting dyad as a model for excess energy dissipation in oxygenic photosynthesis, Proc. Natl. Acad. Sci. U. S. A. 103 (2006) 5343–5348.
[7] N.E. Holt, D. Zigmantas, L. Valkunas, X.-P. Li, K.K. Niyogi, G.R. Fleming, Carotenoid cation formation and the regulation of photosynthetic light harvesting, Science 307 (2005) 433–436 (80-.).
[8] Y. Miloslavina, A. Wehner, P.H. Lambrev, E. Wientjes, M. Reus, G. Garab, et al., Far-red fluorescence: a direct spectroscopic marker for LHCII oligomer formation in non-photochemical quenching, FEBS Lett. 582 (2008) 3625–3631.
[9] M. Wahadoszamen, R. Berera, A.M. Ara, E. Romero, R. van Grondelle, Identification of two emitting sites in the dissipative state of the major light harvesting antenna, Phys. Chem. Chem. Phys. 14 (2012) 759–766.
[10] R. Berera, M. Gwizdala, I.H.M. van Stokkum, D. Kirilovsky, R. van Grondelle, Excited states of the inactive and active forms of the orange carotenoid protein, J. Phys. Chem. B 117 (2013) 9121–9128.
[11] M. Wahadoszamen, A. Ghazaryan, H.E. Cingil, A.M. Ara, C. Büchel, R. van Grondelle, et al., Stark fluorescence spectroscopy reveals two emitting sites in the dissipative state of FCP antennas, Biochim. Biophys. Acta Bioenerg. 1837 (2014) 193–200.
[12] C. Wilhelm, C. Buchel, J. Fisahn, R. Goss, T. Jakob, J. LaRoche, et al., The regulation of carbon and nutrient assimilation in diatoms is significantly different from green algae, Protist 157 (2006) 91–124.
[13] C. Buchel, Fucoxanthin–chlorophyll proteins in diatoms: 18 and 19 kDa subunits assemble into different oligomeric states, Biochemistry 42 (2003) 13027–13034.
[14] L. Premvardhan, B. Robert, A. Beer, C. Buchel, Pigment organization in fucoxanthin chlorophyll a/c(2) proteins (FCP) based on resonance Raman spectroscopy and sequence analysis, Biochim. Biophys. Acta Bioenerg. 1797 (2010) 1647–1656.
[15] E. Papagiannakis, I.H.M. van Stokkum, H. Fey, C. Buchel, R. van Grondelle, Spectroscopic characterization of the excitation energy transfer in the fucoxanthin–chlorophyll protein of diatoms, Photosynth. Res. 86 (2005) 241–250.
[16] M. Olaizola, J. Roche, Z. Kolber, P.G. Falkowski, Non-photochemical fluorescence quenching and the diadinoxanthin cycle in a marine diatom, Photosynth. Res. 41 (1994) 357–370.
[17] B. DemmigAdams, W.W. Adams, The role of xanthophyll cycle carotenoids in the protection of photosynthesis, Trends Plant Sci. 1 (1996) 21–26.
[18] J. Lavaud, B. Rousseau, H.J. van Gorkom, A.-L. Etienne, Influence of the diadinoxanthin pool size on photoprotection in the marine planktonic diatom *Phaeodactylum tricornutum*, Plant Physiol. 129 (2002) 1398–1406.
[19] A. Beer, K. Gundermann, J. Beckmann, C. Büchel, Subunit composition and pigmentation of fucoxanthin–chlorophyll proteins in diatoms: evidence for a subunit involved in diadinoxanthin and diatoxanthin binding†, Biochemistry 45 (2006) 13046–13053.
[20] D. Zigmantas, R.G. Hiller, F.P. Sharples, H.A. Frank, V. Sundstrom, T. Polivka, Effect of a conjugated carbonyl group on the photophysical properties of carotenoids, Phys. Chem. Chem. Phys. 6 (2004) 3009–3016.
[21] L. Premvardhan, D.J. Sandberg, H. Fey, R.R. Birge, C. Buchel, R. van Grondelle, The charge-transfer properties of the S-2 state of fucoxanthin in solution and in fucoxanthin chlorophyll-a/c(2) protein (FCP) based on stark spectroscopy and molecular-orbital theory, J. Phys. Chem. B 112 (2008) 11838–11853.
[22] B. Bailleul, A. Rogato, A. de Martino, S. Coesel, P. Cardol, C. Bowler, et al., An atypical member of the light-harvesting complex stress-related protein family modulates diatom responses to light, Proc. Natl. Acad. Sci. U. S. A. 107 (2010) 18214–18219.
[23] K. Gundermann, C. Buchel, The fluorescence yield of the trimeric fucoxanthin–chlorophyll–protein FCPa in the diatom Cyclotella meneghiniana is dependent on the amount of bound diatoxanthin, Photosynth. Res. 95 (2008) 229–235.
[24] K. Gundermann, C. Büchel, Factors determining the fluorescence yield of fucoxanthin–chlorophyll complexes (FCP) involved in non-photochemical quenching in diatoms, Biochim. Biophys. Acta Bioenerg. 1817 (2012) 1044–1052.
[25] A. Ruban, J. Lavaud, B. Rousseau, G. Guglielmi, P. Horton, A.-L. Etienne, The super-excess energy dissipation in diatom algae: comparative analysis with higher plants, Photosynth. Res. 82 (2004) 165–175.
[26] A.V. Ruban, D. Rees, G.D. Noctor, A. Young, P. Horton, Long-wavelength chlorophyll species are associated with amplification of high-energy-state excitation quenching in higher-plants, Biochim. Biophys. Acta 1059 (1991) 355–360.
[27] T.G. Owens, Light-harvesting function in the diatom phaeodactylum tricornutum: II. Distribution of excitation energy between the photosystems, Plant Physiol. 80 (1986) 739–746.
[28] C.S. Ting, T.G. Owens, The effects of excess irradiance on photosynthesis in the marine diatom *Phaeodactylum tricornutum*, Plant Physiol. 106 (1994) 763–770.
[29] Y. Miloslavina, I. Grouneva, P.H. Lambrev, B. Lepetit, R. Goss, C. Wilhelm, et al., Ultra-fast fluorescence study on the location and mechanism of non-photochemical quenching in diatoms, Biochim. Biophys. Acta Bioenerg. 1787 (2009) 1189–1197.
[30] B. Lepetit, D. Volke, M. Gilbert, C. Wilhelm, R. Goss, Evidence for the existence of one antenna-associated, lipid-dissolved and two protein-bound pools of diadinoxanthin cycle pigments in diatoms, Plant Physiol. 154 (2010) 1905–1920.
[31] N. Gildenhoff, S. Amarie, K. Gundermann, A. Beer, C. Buchel, J. Wachtveitl, Oligomerization and pigmentation dependent excitation energy transfer in fucoxanthin–chlorophyll proteins, Biochim. Biophys. Acta Bioenerg. 1797 (2010) 543–549.

[32] N. Gildenhoff, J. Herz, K. Gundermann, C. Buchel, J. Wachtveitl, The excitation energy transfer in the trimeric fucoxanthin–chlorophyll protein from *Cyclotella meneghiniana* analyzed by polarized transient absorption spectroscopy, Chem. Phys. 373 (2010) 104–109.

[33] F.A. Depauw, A. Rogato, M. Ribera d'Alcalá, A. Falciatore, Exploring the molecular basis of responses to light in marine diatoms, J. Exp. Bot. 63 (2012) 1575–1591.

[34] I. Grouneva, T. Jakob, C. Wilhelm, R. Goss, A new multicomponent NPQ mechanism in the diatom *Cyclotella meneghiniana*, Plant Cell Physiol. 49 (2008) 1217–1225.

[35] R. Nagao, M. Yokono, S. Akimoto, T. Tomo, High excitation energy quenching in fucoxanthin chlorophyll a/c-binding protein complexes from the diatom *Chaetoceros gracilis*, J. Phys. Chem. B 117 (2013) 6888–6895.

[36] R. Berera, R. van Grondelle, J.T.M. Kennis, Ultrafast transient absorption spectroscopy: principles and application to photosynthetic systems, Photosynth. Res. 101 (2009) 105–118.

[37] E. Songaila, R. Augulis, A. Gelzinis, V. Butkus, A. Gall, C. Büchel, et al., Ultrafast energy transfer from chlorophyll c 2 to chlorophyll a in fucoxanthin–chlorophyll protein complex, J. Phys. Chem. Lett. 4 (2013) 3590–3595.

[38] I.H.M. van Stokkum, D.S. Larsen, R. van Grondelle, Global and target analysis of time-resolved spectra, Biochim. Biophys. Acta Bioenerg. 1657 (2004) 82–104.

[39] L. Provasoli, J.J.A. McLaughlin, M.R. Droop, The development of artificial media for marine algae, Arch. Mikrobiol. 25 (1957) 392–428.

[40] T.P.J. Kruger, V.I. Novoderezhkin, C. Ilioaia, R. van Grondelle, Fluorescence spectral dynamics of single LHCII trimers, Biophys. J. 98 (2010) 3093–3101.

[41] T.P.J. Kruger, C. Ilioaia, L. Valkunas, R. van Grondelle, Fluorescence intermittency from the main plant light-harvesting complex: sensitivity to the local environment, J. Phys. Chem. B 115 (2011) 5083–5095.

[42] H.A. Frank, R.J. Cogdell, Carotenoids in photosynthesis, Photochem. Photobiol. 63 (1996) 257–264.

[43] A. Osuka, T. Kume, G.W. Haggquist, T. Jávorfi, J.C. Lima, E. Melo, et al., Photophysical characteristics of two model antenna systems: a fucoxanthin–pyropheoporbide dyad and its peridinin analogue, Chem. Phys. Lett. 313 (1999) 499–504.

[44] M. Di Valentin, C. Büchel, G.M. Giacometti, D. Carbonera, Chlorophyll triplet quenching by fucoxanthin in the fucoxanthin–chlorophyll protein from the diatom *Cyclotella meneghiniana*, Biochem. Biophys. Res. Commun. 427 (2012) 637–641.

[45] M. Di Valentin, E. Meneghin, L. Orian, A. Polimeno, C. Büchel, E. Salvadori, et al., Triplet–triplet energy transfer in fucoxanthin–chlorophyll protein from diatom *Cyclotella meneghiniana*: insights into the structure of the complex, Biochim. Biophys. Acta Bioenerg. 1827 (2013) 1226–1234.

[46] M. Kloz, S. Pillai, G. Kodis, D. Gust, T.A. Moore, A.L. Moore, et al., Carotenoid photoprotection in artificial photosynthetic antennas, J. Am. Chem. Soc. 133 (2011) 7007–7015.

[47] P. Horton, A.V. Ruban, D. Rees, A.A. Pascal, G. Noctor, A.J. Young, Control of the light-harvesting function of chloroplast membranes by aggregation of the LHCII chlorophyll protein complex, FEBS Lett. 292 (1991) 1–4.

[48] Y. Tang, X. Wen, Q. Lu, Z. Yang, Z. Cheng, C. Lu, Heat stress induces an aggregation of the light-harvesting complex of photosystem II in spinach plants, Plant Physiol. 143 (2007) 629–638.

[49] P. Jahns, A.R. Holzwarth, The role of the xanthophyll cycle and of lutein in photoprotection of photosystem II, Biochim. Biophys. Acta Bioenerg. 1817 (2012) 182–193.

[50] R. Berera, I.H.M. van Stokkum, S. D'Haene, J.T.M. Kennis, R. van Grondelle, J.P. Dekker, A mechanism of energy dissipation in cyanobacteria, Biophys. J. 96 (2009) 2261–2267.

[51] D. Kosumi, K. Abe, H. Karasawa, M. Fujiwara, R.J. Cogdell, H. Hashimoto, et al., Ultrafast relaxation kinetics of the dark S1 state in all-trans-β-carotene explored by one- and two-photon pump–probe spectroscopy, Chem. Phys. 373 (2010) 33–37.

[52] M. Szabó, L. Premvardhan, B. Lepetit, R. Goss, C. Wilhelm, G. Garab, Functional heterogeneity of the fucoxanthins and fucoxanthin–chlorophyll proteins in diatom cells revealed by their electrochromic response and fluorescence and linear dichroism spectra, Chem. Phys. 373 (2010) 110–114.